

## Synthesis of Pyranopyrazoles Using Magnetically Recyclable Heterogeneous Iron Oxide-silica Core-shell Nanocatalyst

Ebrahim Soleimani,<sup>a\*</sup> Mohammad Jafarzadeh,<sup>a\*</sup> Parastoo Norouzi,<sup>a</sup> Jedol Dayou,<sup>b</sup>  
Coswald Stephen Sipaut,<sup>c</sup> Rachel Fran Mansa<sup>c</sup> and Parisa Saei<sup>a</sup>

<sup>a</sup>Faculty of Chemistry, Razi University, Kermanshah 67149-67346, Iran

<sup>b</sup>Faculty of Science and Natural Resources, Universiti Malaysia Sabah, 88400 Kota Kinabalu, Sabah, Malaysia

<sup>c</sup>Faculty of Engineering, Universiti Malaysia Sabah, UMS Road, 88400, Kota Kinabalu, Sabah, Malaysia

(Received: Sept. 14, 2014; Accepted: Oct. 28, 2015; Published Online: Dec. 14, 2015; DOI: 10.1002/jccs.201400387)

The Fe<sub>3</sub>O<sub>4</sub>@SiO<sub>2</sub> core-shell nanocatalyst were prepared and efficiently used for four-component coupling reaction of aromatic aldehydes, malononitrile, ethyl acetoacetate and hydrazine hydrate in water/ethanol mixture. Various aromatic aldehydes possessing electron-withdrawing and electron-donating groups in different positions on the ring were successfully transformed to substituted pyranopyrazoles in high yields in short time. The nanocatalyst was easily recovered, and reused five times without significant loss in catalytic activity and performance. The structure, size and morphology of the nanosized catalyst were studied by various techniques such as Fourier transform infrared spectroscopy, powder X-ray diffraction, dynamic light scattering and transmission electron microscopy.

**Keywords:** Pyranopyrazole; Multi-component reactions; Nanocatalyst; Core-shell; Silica.

### INTRODUCTION


Pyranopyrazoles have found remarkable attention for the synthesis of promising biologically significant compounds.<sup>1</sup> They exhibit appreciable biological activities such as analgesic, anti-tumor, anti-cancer, and anti-inflammatory properties, and also serve as potential inhibitors of human Chk1 kinase.<sup>1</sup> There have been reported some catalytic system, homogeneous and heterogeneous, for the preparation of pyrano[2,3-c]pyrazol-6-ones via multicomponent reactions, such as  $\gamma$ -alumina,<sup>1</sup> Mg/Al hydrotalcite,<sup>2</sup> MgO nanoparticle,<sup>3</sup> H<sub>4</sub>SiW<sub>12</sub>O<sub>40</sub>,<sup>4</sup> Ba(OH)<sub>2</sub>,<sup>5</sup> silica gel 60,<sup>6</sup> trichloroacetic acid,<sup>7</sup> ceric sulfate,<sup>7</sup> ZnO nanoparticle,<sup>8</sup> L-proline,<sup>9</sup> per-6-amino- $\beta$ -cyclodextrin.<sup>10</sup> Some of the reported methods suffer high reaction temperature, poor catalyst recoverability, and in some cases tedious procedure for catalyst recyclability and low reusability. Magnetic-assisted in recyclability of the catalyst can efficiently overcome the difficulty of catalyst recoverability.

Nanoparticulate heterogeneous solid catalysts have received considerable attention in organic transformations compared to their corresponding bulk materials in term of their ability to accelerate the rates of reactions, high catalytic activity, reusability and higher yield of products which is due to their high surface area-to-volume ratio and large specific surface area.<sup>11,12</sup> The available surface area

of the nanocatalysts is important factor as the number of contact between the reactant molecules and catalyst significantly increased. It is expected that the catalytic activity of heterogeneous nanocatalysts efficiently enhanced comparable with its homogeneous counterpart. The size of the nanocatalysts is important due to providing a highly active catalyst surface, which maximizes the reaction rates and minimizes consumption of the catalyst.<sup>13</sup> In addition, because of effectiveness of the active site of nanocatalyst, the smaller amount of catalyst can be used that could lead to limited usage of the catalyst.

Silica is one of the best inorganic heterogeneous materials for organic transformations. It has exceptional thermal and chemical stability in the presence of majority of chemicals, except bases, and it is also an abundant and inexpensive material.<sup>14</sup> The sol-gel process as a wet chemical method is commonly applied for the fabrication of silica through hydrolysis and condensation of corresponding alkoxides and inorganic salts.<sup>15</sup> A main feature of silica is the existence of porosity within the silica structure. Porosity introduces a large surface area inside the silica particles.<sup>16,17</sup> They are usually used for preparation of magnetite-silica core-shell nanoparticles by coating of magnetite (Fe<sub>3</sub>O<sub>4</sub>) surface with silica because of the strong affinity of iron oxide surfaces toward silica.<sup>18</sup> Many efforts have been devoted in the con-

\* Corresponding author. Email: mjafarzadeh1027@yahoo.com; e\_soleimanirazi@yahoo.com

 Supporting information for this article is available on the www under <http://dx.doi.org/10.1002/jccs.201400387>

trolled synthesis of iron oxide/SiO<sub>2</sub> in literature.<sup>19-21</sup> The use of magnetic nanoparticles as a catalyst support can also enable easy and efficient separation of the catalysts from the reaction mixture with an external magnet.<sup>22</sup>

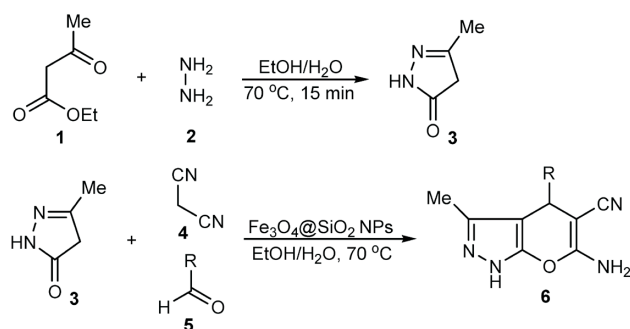
The aim of this research is applying magnetically separable nanocatalyst, Fe<sub>3</sub>O<sub>4</sub>@SiO<sub>2</sub> core-shell nanoparticles (NPs), for the synthesis of pyrazoles. The catalytic capability and reusability of the catalyst were also investigated.

## RESULTS AND DISCUSSION

### Catalytic reaction

Scheme 1 exhibits the application of magnetic heterogeneous nanocatalysts for the synthesis of pyranopyrazoles. Fe<sub>3</sub>O<sub>4</sub>-supported SiO<sub>2</sub> NPs can be enabled to easily separate from the reaction mixture by an external magnet and reused several times. Silica, as a non-toxic catalyst, can be easily regenerated through rinsing with ethanol and dried in oven overnight. Due to the nano-size of silica, large surface area, high porosity and high number of active functional groups (silanol: Si-OH)<sup>23</sup> can be available on the surface of the catalyst. High quantity of active sites in silica shell is expected to show good catalytic activity in organic reactions. High dispersity and homogeneity of nanocatalyst in reaction medium can also affect on the catalyst reactivity.

**Scheme 1** Synthesis of pyranopyrazoles



The catalytic activity of the Fe<sub>3</sub>O<sub>4</sub>@SiO<sub>2</sub> NPs was investigated in the synthesis of pyranopyrazoles. The reaction between hydrazine hydrate, ethyl acetoacetate (EAA), malononitrile and benzaldehyde was chosen as a model condensation reaction. For optimizing the reaction condition, the reaction was initially carried out in the presence of 0.1 g Fe<sub>3</sub>O<sub>4</sub>@SiO<sub>2</sub> NPs at room temperature in water. The results showed that the reaction was not completed even after 4-5 h. Therefore, heating up the mixture of ethyl

acetoacetate and hydrazine hydrate, and using of water/ethanol (50:50 v:v%) mixture as a medium were applied. 4-chlorobenzaldehyde and malononitrile were then added into the mixture in the presence of Fe<sub>3</sub>O<sub>4</sub>@SiO<sub>2</sub> NPs (0.075 g) for 25 min which afforded in 70% yield (Table 1, Entry 1). The elevated temperature was required to accelerate the reaction rate. Moreover, decrease in polarity of the solvent by addition of ethanol to water facilitated the dissolution of the reactants in the solvent and homogenized the reaction medium. Therefore, temperature and solvent composition were two effective parameters to achieve higher yield within shorter time. The same reaction condition with 0.1 g of the catalyst gave an increased yield of 90% (Table 1, Entry 2). By varying the amount of the catalyst, the optimized value was obtained at 0.2 g which resulted in 94% yield (Table 1, Entry 3). Further increase in the amount of the catalyst was not efficient. It might be due to high agglomeration and low dispersity of the catalyst in the reaction medium that leads to decrease in the number of active sites (Table 1, Entry 4). Using non-toxic catalyst and avoid to use organic and volatile solvent provide a mild reaction condition for this approach.

The catalytic system was further extended to the synthesis of various pyranopyrazoles, as hydrazine hydrate, ethyl acetoacetate (EAA), malononitrile and variety of benzaldehyde were used under the optimized reaction conditions. The resulting products with yield of synthesis and time of reaction completion are presented in Table 2. Almost all the employed aldehydes were smoothly preceded the reactions towards the desired products in good yields ir-

**Table 1.** Optimization of the reaction condition with 4-chlorobenzaldehyde using different amount of Fe<sub>3</sub>O<sub>4</sub>@SiO<sub>2</sub> NPs

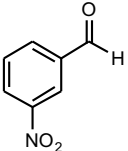
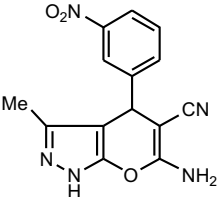
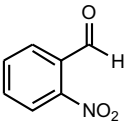
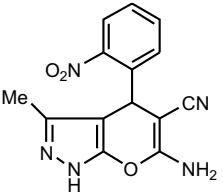
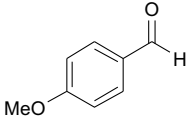
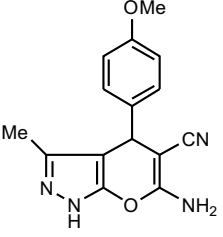
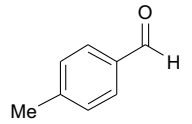
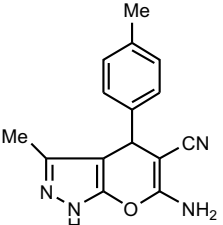
Entry	Reaction condition	Yield (%) <sup>a</sup>
1	Fe <sub>3</sub> O <sub>4</sub> @SiO <sub>2</sub> (0.075 g), 25 min, 70 °C	70
2	Fe <sub>3</sub> O <sub>4</sub> @SiO <sub>2</sub> (0.1 g), 25 min, 70 °C	90
3	Fe <sub>3</sub> O <sub>4</sub> @SiO <sub>2</sub> (0.2 g), 25 min, 70 °C	94
4	Fe <sub>3</sub> O <sub>4</sub> @SiO <sub>2</sub> (0.3 g), 25 min, 70 °C	70

<sup>a</sup> Reaction conditions: Ethyl acetoacetate (1 mmol), hydrazine hydrate (1 mmol), 4-chlorobenzaldehyde (1 mmol), malononitrile (1 mmol) in water/ethanol mixture (1 mL).

<sup>b</sup> Isolated yields.

Table 2. Synthesis of pyranopyrazoles from various aromatic aldehydes, malononitrile, ethyl acetoacetate and hydrazine hydrate in the presence of Fe<sub>3</sub>O<sub>4</sub>@SiO<sub>2</sub> core-shell NPs<sup>a</sup>

Entry	Aldehydes	Product	Time (min)	Yield (%)	mp (°C)	
					Found	Reported
1			35	85	242-246	(243-245) <sup>8</sup>
2			25	94	233-234	(233-235) <sup>8</sup>
3			30	90	144-147	(145-147) <sup>1</sup>
4			20	92	177-180	(180-183) <sup>22</sup>
5			30	80	222-226	(224-226) <sup>1</sup>
6			30	94	249-253	(251-253) <sup>1</sup>

7			35	90	193-195	(190-192) <sup>22</sup>
8			40	88	218-221	(220-222) <sup>1</sup>
9			30	83	209-211	(210-212) <sup>1</sup>
10			20	84	205-208	(206-207) <sup>8</sup>

<sup>a</sup> Reaction conditions: Ethyl acetoacetate (1 mmol), hydrazine hydrate (1 mmol), various aromatic aldehydes (1 mmol), malononitril (1 mmol) and Fe<sub>3</sub>O<sub>4</sub>@SiO<sub>2</sub> (0.2 g).

<sup>b</sup> Isolated yield.

<sup>c</sup> Data from literature [1,8,22].

respective of the presence of electron withdrawing or donating substituents in the *ortho*, *meta* or *para* positions on the ring of various aromatic aldehydes. The results are also revealed that high yields of the products were obtained for the electron-withdrawing benzaldehydes, such as 2-nitrobenzaldehyde, 3-nitrobenzaldehyde and 4-nitrobenzaldehyde aldehydes (Table 2, Entries 6-8). In addition, this reaction was affected by steric effect. For example, 2-nitrobenzaldehyde (Table 2, Entry 8) required longer reaction time compared to 4-nitrobenzaldehyde (Table 2, Entry 6) due to sterically hindered effect of *ortho* position.

The reusability of the Fe<sub>3</sub>O<sub>4</sub>@SiO<sub>2</sub> nanocatalyst was evaluated by using the reaction of 4-chlorobenzaldehyde as a model reaction. The catalyst was recovered by simple applying an external magnetic field and washed with boiling ethanol. The resulting catalyst was further used for the reaction in several runs. Fe<sub>3</sub>O<sub>4</sub>@SiO<sub>2</sub> NPs were remained active even after 5 repeated cycles of each reaction. The re-

sults showed that this catalyst could be reusable several times without loss of activity in the reaction. These results are summarized in Figure 1. The loss of activity might be related to the agglomeration among core-shell nanoparticles, as the layer of silica with silanol groups is susceptible for aggregation and agglomeration with silanols in neighboring particles. Decrease in specific surface area arising from the agglomeration is generally main reason in decreasing the number of active sites on the surface of Fe<sub>3</sub>O<sub>4</sub>@SiO<sub>2</sub> NPs.

To extend the synthetic methodology for pyranopyrazoles, the monodisperse SiO<sub>2</sub> nanoparticles with average size of 10 nm (prepared according to our previous work<sup>23</sup>) were utilized as a catalyst to promote the rate and yield of the reaction. The results were exhibited similar trend to the results of using the Fe<sub>3</sub>O<sub>4</sub>@SiO<sub>2</sub> NPs, however Fe<sub>3</sub>O<sub>4</sub>@SiO<sub>2</sub> NPs were more efficient in catalytic activity compared to the SiO<sub>2</sub> NPs. Moreover, SiO<sub>2</sub> NPs showed good catalytic activity even after five times recycle and reuse.

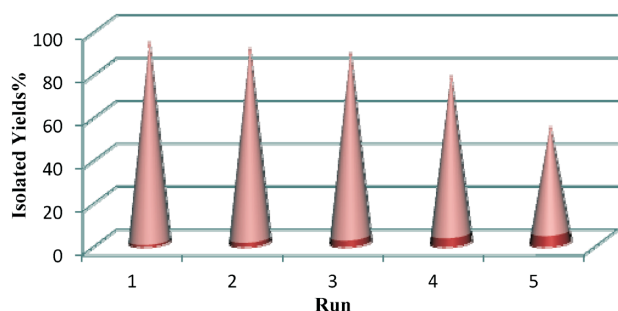


Fig. 1. The catalytic activity of recycled Fe<sub>3</sub>O<sub>4</sub>@SiO<sub>2</sub> NPs in a model reaction with 4-chlorobenzaldehyde.

### Preparation and characterization of the nanocatalyst

Magnetic NPs have found great applications due to rapidly and easily separation from reaction media using a magnetic field.<sup>22</sup> Magnetite (Fe<sub>3</sub>O<sub>4</sub>) NPs were prepared via a chemical co-precipitation of Fe<sup>2+</sup> and Fe<sup>3+</sup> ions in basic solution,<sup>20</sup> and then silica was coated onto the surface of the Fe<sub>3</sub>O<sub>4</sub> NPs by sol-gel process through hydroxyl groups in the aqueous medium. The formation of silica was involved the hydrolysis and condensation of alkoxy silanes in ethanol, in the presence of water and ammonia.<sup>24</sup> This procedure was expected to give the NPs with better dispersion and less agglomeration and aggregation because the growth of silica layer took place on the surface of magnetite NPs.

The crystalline of Fe<sub>3</sub>O<sub>4</sub> NPs before and after silica coating, were identified with XRD technique (Fig. 2). For Fe<sub>3</sub>O<sub>4</sub> NPs, diffraction peaks with 2θ at 30°, 35.5°, 43°, 53.8°, 56.9° and 62.5° were referred to [220], [311], [400], [422], [511], and [440] planes of cubic spinel of Fe<sub>3</sub>O<sub>4</sub>, respectively. The results are in good agreement with the XRD patterns of Fe<sub>3</sub>O<sub>4</sub> NPs reported previously.<sup>25</sup> The (311) XRD peak was used to estimate the size of crystallite of magnetite using Scherrer's formula;  $D = 0.9\lambda / (\beta \cos\theta)$ , where D is the average crystalline size, λ is wavelength of X-ray source (Cu Kα, 1.54 Å), β is the angular line width of half-maximum intensity (full width at the half-maximum; FWHM) and θ is Bragg's diffraction angle in degree. The mean crystallite size calculated to be about 27 nm. After silica coating, no change observed in the crystalline structure of the Fe<sub>3</sub>O<sub>4</sub> core (Figure 2b). The broad peak at 2θ of 22° corresponded to the amorphous nature of the silica shell. Silica-coated iron oxide NPs still maintain the magnetization characteristics of the bare Fe<sub>3</sub>O<sub>4</sub> NPs.

The Fourier Transform Infrared (FTIR) spectrum of Fe<sub>3</sub>O<sub>4</sub>@SiO<sub>2</sub> NPs in Figure 3 exhibits an absorption peak at

3250 cm<sup>-1</sup>, which is the characteristic peak of OH stretching vibration and is also indicated to the presence of some amount of ferric hydroxide in Fe<sub>3</sub>O<sub>4</sub>. The three distinct absorption peaks at 893 cm<sup>-1</sup>, 634 cm<sup>-1</sup>, and 564 cm<sup>-1</sup> are characteristic vibrations of spinel and attributed to the vibrations of Fe<sup>2+</sup>-O and Fe<sup>3+</sup>-O, respectively.<sup>20</sup> The sharp and high intense peak appears at ~880 cm<sup>-1</sup> demonstrates high degree of crystallinity in the Fe<sub>3</sub>O<sub>4</sub> NPs.<sup>26</sup> This characteristic absorption band therefore confirm the existence of crystal phase in Fe<sub>3</sub>O<sub>4</sub>. On the other hand, the absorption bands at 3450 cm<sup>-1</sup>, 1100 cm<sup>-1</sup>, and 952 cm<sup>-1</sup> corresponded to the stretching, asymmetric stretching and bending of silanols groups (Si-OH) on the silica surface, respectively. Intensive bands at 1100–1200 cm<sup>-1</sup> and 473 cm<sup>-1</sup> repre-

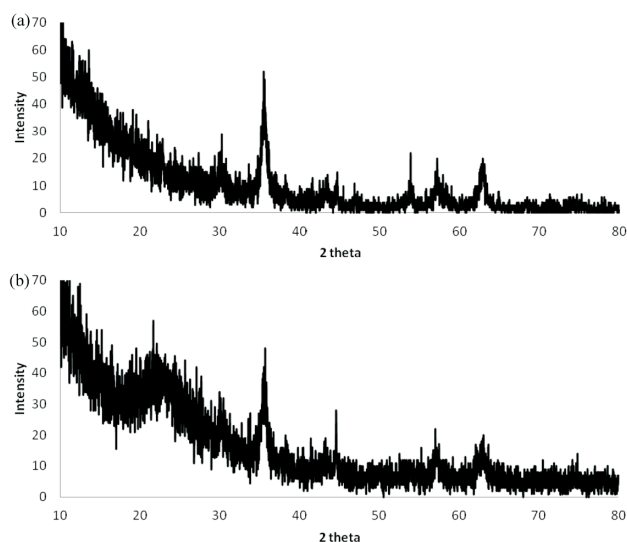


Fig. 2. XRD patterns of (a) Fe<sub>3</sub>O<sub>4</sub> and (b) Fe<sub>3</sub>O<sub>4</sub>@SiO<sub>2</sub> NPs.

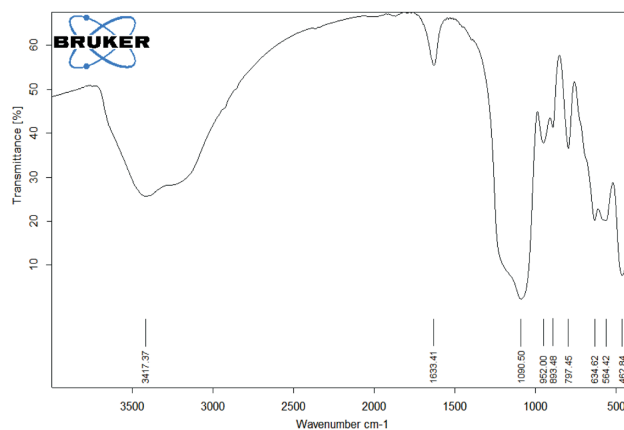


Fig. 3. FT-IR spectrum of Fe<sub>3</sub>O<sub>4</sub>@SiO<sub>2</sub> NPs.



sented the asymmetric stretching and bending of siloxane groups (Si–O–Si). Vibrations at  $3500\text{--}3400\text{ cm}^{-1}$ ,  $1633\text{ cm}^{-1}$ , and  $797\text{ cm}^{-1}$  assigned to the adsorbed water (H–OH, stretching vibration), residual intermolecular water (H–OH, bending) and moisture (H–OH, bending) in the samples.<sup>23</sup>

The study on the particle size and particle size distribution (PSD) of  $\text{Fe}_3\text{O}_4$  and  $\text{Fe}_3\text{O}_4@\text{SiO}_2$  NPs were performed using dynamic light scattering (DLS) (Figure 4). The Z-average particle size of  $\text{Fe}_3\text{O}_4$  NPs and  $\text{Fe}_3\text{O}_4@\text{SiO}_2$  NPs in ethanol were found to be  $\sim 174\text{ nm}$  (87 r.nm; radius nanometer, PDI = 1.000) and  $\sim 306$  (153 r.nm; radius nanometer, PDI = 1.000), respectively. The particle size is defined as an average hydrodynamic diameter indicating the aggregation phenomenon within nanoparticles. Moreover, the uniformity and homogeneity in particle size is inferred from narrow particle size distribution. A difference between the DLS and XRD sizes is observed the size calculated by XRD was related to the size of crystallites, whereas DLS gave the size of aggregated and agglomerated particles.

The morphology of  $\text{Fe}_3\text{O}_4@\text{SiO}_2$  NPs was studied by Transmission Electron Microscopy (TEM). Figure 5 shows that the  $\text{Fe}_3\text{O}_4$  NPs were roughly spherical with agglomeration within the nanoparticles. The silica layer was then coated on the surface of the groups of iron oxides nanoparticles. Although upon the formation of silica shell on the surface of  $\text{Fe}_3\text{O}_4$  NPs, the magnetic property of the  $\text{Fe}_3\text{O}_4@$

$\text{SiO}_2$  NPs was decreased, but the core-shell system exhibited sufficient magnetic response to the external magnetic force during magnetically isolation of the catalyst from the reaction medium.

## CONCLUSIONS

The potential application of  $\text{Fe}_3\text{O}_4@\text{SiO}_2$  core-shell nanocatalysts was studied for the synthesis of pyranopyrazole via a one-pot four-component reaction of hydrazine hydrate, ethyl acetoacetate (EAA), malononitrile and various aromatic aldehydes in aqueous medium. The corresponding products were synthesized in good to excellent yield in short time. The effect of temperature and solvent polarity on the reactions yield and time were also observed. The advantageous of the current work can be noted: easy preparation and handling of the environmental benign catalyst, simplicity in operation of the one-pot reaction, and mild reaction condition. Furthermore, a simple and fast recycling of the catalyst from the reaction medium without any tedious work-up or extensive purification were other great features of this synthetic method. The catalyst was durable, and successfully reused for at least five times without significant loss in catalytic activity. Finally, employing magnetically recyclable catalyst can avoid solvent and energy consumption during its recovery, and make it a cost-effective catalyst.

## EXPERIMENTAL

Chemicals were purchased from Fluka and Merck chemical companies. All synthesized products were identified using FTIR and  $^1\text{H}$  NMR, and then verified in comparison with reported data

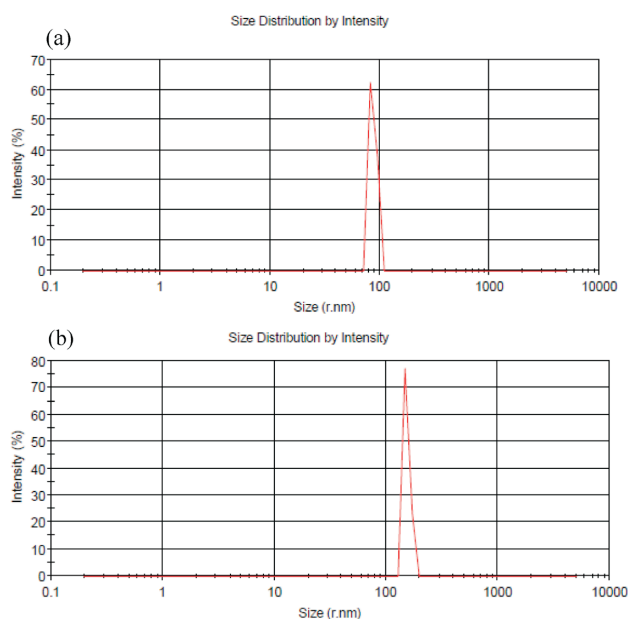


Fig. 4. Particle size distribution of (a)  $\text{Fe}_3\text{O}_4$  and (b)  $\text{Fe}_3\text{O}_4@\text{SiO}_2$  NPs obtained by DLS.

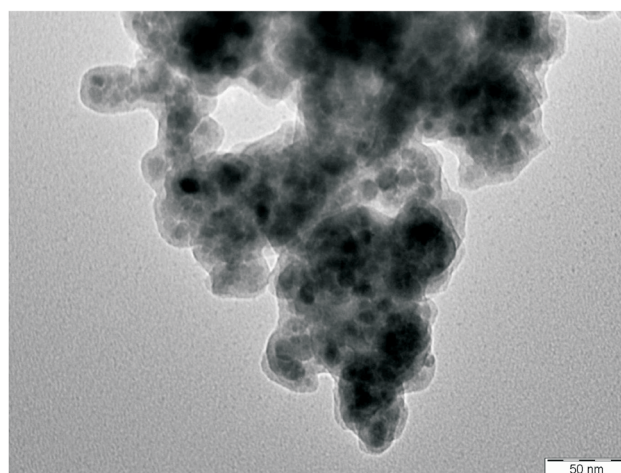


Fig. 5. TEM image of  $\text{Fe}_3\text{O}_4@\text{SiO}_2$  NPs.

in literature (see Supplementary data).

**Typical procedure for the preparation of Fe<sub>3</sub>O<sub>4</sub> nanoparticles:** Fe<sub>3</sub>O<sub>4</sub> nanoparticles (NPs) were synthesized by a chemical co-precipitation method.<sup>20</sup> Aqueous solution of FeCl<sub>3</sub> and FeCl<sub>2</sub> in a molar ratio of Fe<sup>2+</sup>/Fe<sup>3+</sup> = 1/2 was prepared and kept at room temperature. For this purpose, 0.036 mol of FeCl<sub>3</sub>·6H<sub>2</sub>O and 0.018 mol of FeCl<sub>2</sub>·4H<sub>2</sub>O were dissolved in 20 mL deionized water under nitrogen gas with vigorous stirring. Then, 25% NH<sub>3</sub> was added into the solution until the pH of the solution reached to 11 and the stirring was continued for 1 h at 60 °C. The color of bulk solution turned from orange to black immediately. The magnetite precipitate was separated from the solution by magnetic decantation, then washed with deionized water and ethanol several times, and finally dried at air.

**Typical procedure for the preparation of core-shell Fe<sub>3</sub>O<sub>4</sub>@SiO<sub>2</sub> nanocatalyst:** An appropriate amount of as-prepared Fe<sub>3</sub>O<sub>4</sub> NPs (45 mg) were initially dispersed in water (16 mL) under ultrasonic irradiation, then an aqueous ammonia solution (25 wt.%, 2 mL) and ethanol (solvent, 80 mL) were added into the dispersed magnetite solution. Tetraethylorthosilicate (TEOS, 0.8 mL) was added dropwise into the solution of Fe<sub>3</sub>O<sub>4</sub> NPs, and the medium was vigorously stirred for 24 h at room temperature. Finally, the core-shell nanocatalyst was collected from the solution by applying an external magnetic force, washed with water and ethanol several times, and dried at 50 °C overnight.

**Typical procedure for the synthesis of pyranopyrazole from four components in the presence of Fe<sub>3</sub>O<sub>4</sub>@SiO<sub>2</sub> nanocatalyst:** In a round-bottomed flask (50 mL), ethyl acetoacetate (1 mmol) was added to hydrazine hydrate (1 mmol) in 50:50 v:v% of water and ethanol (1 mL) and the solution was heated at 70 °C in an oil bath under violent stirring for 15 min. After the formation of light solution, followed by adding various aromatic aldehydes (1 mmol) and malononitrile (1 mmol) in the presence of the catalyst (0.2 g), stirring was continued for 20-50 min at 70 °C in the oil bath. Completion of the reaction was monitored by TLC. The reaction mass was allowed to cool and then the catalyst was isolated by applying an external magnet. The solvent was evaporated and product was purified. Furthermore, the recycled catalyst was reused for several times in the synthesis of pyranopyrazoles under same reaction conditions.

**Characterization techniques:** Melting points were determined in open capillaries with a Gallen-Kamp melting point apparatus. Infrared spectra were obtained by using a Ray Leigh Wqf-510 FT-IR spectrophotometer. X-ray diffraction was conducted using Philips x'pert pro X-ray diffractometer (PW 3040), with monochromatic high-intensity Cu-K $\alpha$  radiation ( $k = 1.54056 \text{ \AA}$ , 40 kV, 30 mA) at  $2\theta$  range of 10-80°. The dry samples

in powder form were exposed under the X-ray at room temperature. Particle size and particle size distribution were determined by zetasizer nanoparticle analyzer, Malvern Nano ZS series (Model: ZEN3600) at room temperature. Zetasizer was equipped with Red Laser (HeNe gas laser, maximum output-power: 4 mW, wavelength: 632.8 nm) as light source and avalanche photodiode as detector. Glass cuvette with square aperture was used as a cell. The samples first dissolved in ethanol with 1 wt.% and then sonicated at an ultrasonic bath for 30 min. After that, the dispersant was filtered to separate agglomerated particles. Ultrasonication was also used to remove air bubbles and breakup agglomerated particles. The morphological studies were performed using a TEM (Transmission Electron Microscopy), Philips CM10 operated at 80 KV electron beam accelerating voltage and equipped with a CCD camera. One drop of the sample solution was placed on a copper grid, and the solvent (ethanol) was evaporated in an ambient conditions.

## ACKNOWLEDGEMENTS

The authors are thankful to Razi University and Universiti Malaysia Sabah for financial supports.

## REFERENCES

- Mecadon, H.; Rohman, M. R.; Rajbangshi, M.; Myrboh, B. *Tetrahedron Lett.* **2011**, *52*, 2523-2525.
- Kshirsagar, S. W.; Patil, N. R.; Samant, S. D. *Synth. Commun.* **2011**, *41*, 1320-1325.
- Babaie, M.; Sheibani, H. *Arab. J. Chem.* **2011**, *4*, 159-162.
- Chavan, H. V.; Babar, S. B.; Hoval, R. U.; Bandgar, B. P. *Bull. Korean Chem. Soc.* **2011**, *32*, 3963-3966.
- Azzam, S. H. S.; Pasha, M. A. *Tetrahedron Lett.* **2012**, *53*, 6834-6837.
- Shinde, P. V.; Gujar, J. B.; Shingate, B. B.; Shingare, M. S. *Bull. Korean Chem. Soc.* **2012**, *33*, 1345-1348.
- Karimi-Jaberi, Z.; Shams, M. M. R.; Pooladian, B. *Acta Chim. Solv.* **2013**, *60*, 105-108.
- Tekale, S. U.; Kauthale, S. S.; Jadhav, K. M.; Pawar, R. P. *J. Chem.* **2013**, 840954.
- Mecadon, H.; Rohman, M. R.; Kharbanger, I.; Laloo, B. M.; Kharkongor, I.; Rajbangshi, M.; Myrboh, B. *Tetrahedron Lett.* **2011**, *52*, 3228-3231.
- Kanagaraj, K.; Pitchumani, K. *Tetrahedron Lett.* **2010**, *51*, 3312-3316.
- Polshettiwar, V.; Varma, R. S. *Green Chem.* **2010**, *12*, 743-754.
- Fihri, A.; Bouhara, M.; Nekoueishahraki, B.; Basset, J.-M.; Polshettiwar, V. *Chem. Soc. Rev.* **2011**, *40*, 5181-5203.
- Narayanan, R.; El-Sayed, M. A. *J. Phys. Chem. B* **2005**, *109*, 12663-12676.
- Iller, R. K. *The Chemistry of Silica*; John Wiley & Sons: New

- York, 1979.
15. Hench, L. L.; West, J. K. *Chem. Rev.* **1990**, *90*, 33-72.
  16. Brinker, C. J.; Scherer, G. W. *Sol-gel Science: The Physics and Chemistry of Sol-gel Processing*; Academic Press: San Diego, 1990.
  17. Vansant, E. F.; Voort, P. V. D.; Vrancken, K. C. *Characterization and Chemical Modification of the Silica Surface*; Elsevier: Amsterdam, 1995.
  18. Sun, S.-N.; Wei, C.; Zhu, Z.-Z.; Hou, Y.-L.; Subbu, S. V.; Xu, Z.-C. *Chin. Phys. B* **2014**, *23*, 037503.
  19. Wang, S.; Cao, H.; Gu, F.; Li, C.; Huang, G. *J. Alloy Compd.* **2008**, *457*, 560-564.
  20. Chen, L.; Xu, Z.; Dai, H.; Zhang, S. *J. Alloy Compd.* **2010**, *497*, 221-227.
  21. Zhang, J.; Li, X.; Rosenholm, J. M.; Gu, H.-C. *J. Colloid Interface Sci.* **2011**, *361*, 16-24.
  22. Zhang, Q.; Su, H.; Luo, J.; Wei, Y. *Green Chem.* **2012**, *14*, 201-208.
  23. Rahman, I. A.; Jafarzadeh, M.; Sipaut, C. S. *J. Sol-Gel Sci. Technol.* **2011**, *59*, 63-72.
  24. Stöber, W.; Fink, A.; Bohn, E. *J. Colloid Interface Sci.* **1968**, *26*, 62-69.
  25. Hui, C.; Shen, C.; Tian, J.; Bao, L.; Ding, H.; Li, C.; Tian, Y.; Shi, X.; Gao, H.-J. *Nanoscale* **2011**, *3*, 701-705.
  26. Ahmad, S.; Riaz, U.; Kaushik, A.; Alam, J. *J. Inorg. Organomet. Polym.* **2009**, *19*, 355-360.